Macromolecules

Article

pubs.acs.org/Macromolecules

# Design, Application, and Morphology Study of a New Photovoltaic Polymer with Strong Aggregation in Solution State

Deping Qian,[†,‡,§] Long Ye,[†,§] Maojie Zhang,[†] Yongri Liang,[†] Liangjie Li,[‡] Ye Huang,[†] Xia Guo,[†] Shaoqing Zhang,[†] Zhan'ao Tan,*[,‡] and Jianhui Hou*[,†]

[†]State Key Laboratory of Polymer Physics and Chemistry, Institute of Chemistry, Chinese Academy of Sciences, Beijing 100190 China

[‡]The New and Renewable Energy of Beijing Key Laboratory, School of Renewable Energy, North China Electric Power University, Beijing 102206, China

**ABSTRACT:** A new conjugated polymer based on 5,7-bis(2-ethylhexyl)benzo[1,2-*c*:4,5-*c*′]dithiophene-4,8-dione, named as PBDTBDD, was designed, synthesized, and applied in polymer solar cells (PSCs). A power conversion efficiency (PCE) of 6.67% was obtained from the PBDTBDD/$PC_{61}BM$-based PSC, which is a remarkable result for the PSCs using $PC_{61}BM$ as electron acceptor. The PBDTBDD/$PC_{61}BM$-based device exhibits a narrow absorption band and excellent quantum efficiency in the range from 500 to 700 nm. Furthermore, PBDTBDD shows a strong aggregation effect in solution state, and the study indicates that although the temperature used in solution preparation has little influence on molecular orientation as well as crystallinity of the D/A blend, it plays an important role in forming proper domain size in the blend. This work provides a good example to reveal the correlation between the morphology of the blend films and the processing temperature of the solution preparation. Furthermore, the study in this work suggests an interesting and feasible approach to modulate domain size without changing crystallinity of the blend films in PSCs.

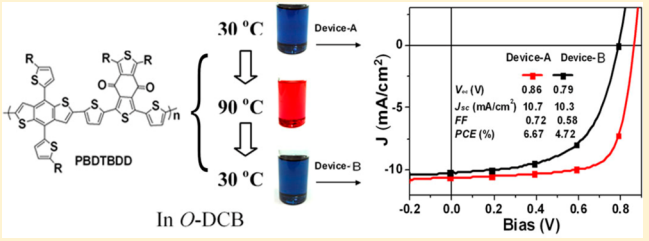


## INTRODUCTION

Great achievements have been made in bulk heterojunction (BHJ) polymer solar cells (PSCs) recently.[1−5] Photovoltaic performance of PSCs can be improved effectively by the applications of new low-band-gap materials.[6−10] Conjugated polymers with strong and broad absorption bands, deep highest occupied molecular orbital (HOMO) levels, and high mobilities have been successfully designed and applied in PSCs, and over 7% efficiencies have been reported by using newly designed materials.[10−14] The morphology of the BHJ blend of an electron donor (such as a conjugated polymer) and an electron acceptor (such as the derivative of fullerene, i.e., phenyl-$C_{61}$-butyric acid methyl ester, $PC_{61}BM$)) is also of great importance to photovoltaic performance of PSCs.[15−18] In order to get efficient photovoltaic performance, forming a bicontinuous interpenetrating network with nanoscale phase separation is necessary, and hence different strategies, such as slow growth,[16] solvent additives,[19] thermal annealing,[16] and postannealing,[20] have been successfully developed and employed to optimize morphology of the BHJ blends. It can be concluded that material design and morphology control are equally important to the study of PSCs.

Aggregation in solution state is an important behavior for conjugated polymers, which is concentration, solvent, and temperature dependent.[21−24] The morphology of the films can be affected by the aggregation of polymer in solution state, and a variety of experiments suggest that the degree of aggregation in solution can be preserved through casting process and affect the morphology of solid films.[23−26] However, how to utilize this process to directly control the morphology of the D/A blends and thus to improve photovoltaic performance of PSCs has been seldom studied.

In this work, a new conjugated polymer, named PBDTBDD based on 1,3-bis(thiophen-2-yl)-5,7-bis(2-ethylhexyl)benzo-[1,2-*c*:4,5-*c*′]dithiophene-4,8-dione (BDD) as shown in Scheme 1, was designed, synthesized, and applied to PSCs. Our results indicate that this new polymer shows promising photovoltaic properties. Interestingly, when *o*-dichlorobenzene (*o*-DCB) is used as solvent, strong aggregation can be observed in the solution of this polymer under ambient temperature (∼30 °C), and the aggregation can be eliminated by heating up the solution to ∼100 °C. Therefore, as demonstrated in Chart 1, two kinds of devices were fabricated. The solution for making device A was prepared under ambient temperature, ca. 30 °C, while the solution for making device B was treated with a heating−cooling process; i.e., the solution was heated up to 90 °C and then cooled down to 30 °C. Then, photovoltaic and morphological properties of the blends were characterized fully. The results indicate that the morphology as well as photovoltaic properties of the devices can be affected by the heating process of solution preparation process. Therefore, we tried to use these data to reveal the correlation between solution preparation

**Received:** September 11, 2012
**Revised:** November 19, 2012
**Published:** December 6, 2012

   dx.doi.org/10.1021/ma301900h | *Macromolecules* 2012, 45, 9611−9617

**Scheme 1. Synthesis and Structure of PBDTBDD**[a]

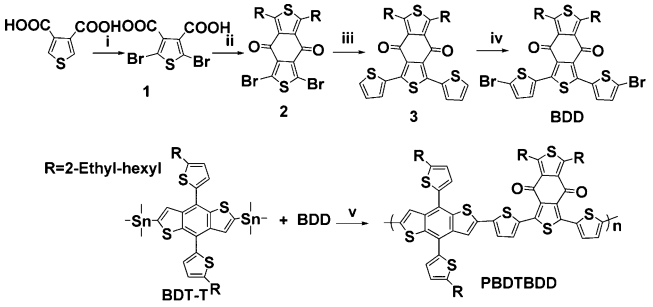


[a]Reagents and conditions: (i) $CH_3COOH$, $Br_2$, stirred overnight; (ii) oxalyl chloride, DMF, 12 h; dichloromethane, 2,5-bis(2-ethylhexyl)-thiophene, $AlCl_3$, ambient temperature, 3 h; (iii) tributyl(thiophen-2-yl)stannane, $[Pd(PPh_3)_4]$, toluene, reflux, 12 h; (iv) DMF, *N*-bromosuccinimide, ambient temperature, 3 h; (v) $[Pd(PPh_3)_4]$, toluene, reflux, 11.5 h.

**Chart 1. Two Device Fabrication Processes of the Polymer Solar Cells Based on the PBDTBDD/$PC_{61}BM$ Blend with a D/A Ratio = 1:1**

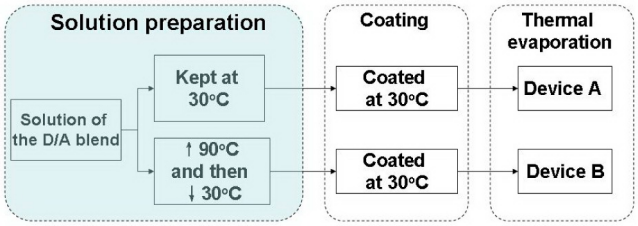


condition and morphology of the D/A (PBDTBDD/$PC_{61}BM$) blend.

## RESULTS AND DISCUSSION

**Synthesis and Characterization of the Polymer.** The synthetic route of PBDTBDD is shown in Scheme 1. Starting with thiophene-3,4-dicarboxylic acid, the BDD monomer can be synthesized through four steps with good yields. Recently, a very similar unit was reported and applied in constructing conjugated polymers.[27] Herein, we replaced hexyl groups on BDD[27] with 2-ethylhexyl groups for good solubility. The polymer was prepared by a Pd-catalyzed Stille coupling reaction and shows good solubility in chloroform and dichlorobenzene. The molecular weight of the polymer is 11.5K ($M_n$) with a PDI of 1.18, which was measured by gel permeation chromatography (GPC) using chloroform as eluent under 45 °C and monodispersed polystyrene as standard. The thermogravimetric analysis (TGA) curve is shown in Figure 1a, and it shows that the polymer exhibits good thermal stability below 350 °C under the inert atmosphere.

**Electrochemical Properties.** Electrochemical cyclic voltammetry (CV) measurement was performed for determining the HOMO and LUMO levels of conjugated polymers.[28] As shown in Figure 1b, both n-doping and p-doping processes of PBDTBDD are reversible. The CV plot of PBDTBDD shows an onset reduction potential ($\varphi_{red}$) at −1.54 V vs $Ag/Ag^+$ and an onset oxidation potential ($\varphi_{ox}$) at 0.51 V vs $Ag/Ag^+$. The HOMO and the LUMO levels as well as the electrochemical band gap ($E_g^{EC}$) of the polymer calculated from $\varphi_{ox}$ and $\varphi_{red}$ are −5.23, −3.18, and 2.05 eV, respectively.[29]

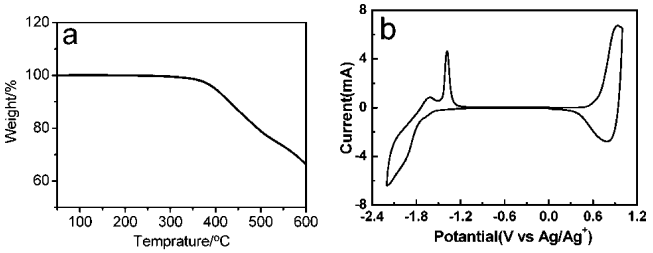


**Figure 1.** (a) TGA plot of the polymer with a heating rate of 10 °C/min under the inert atmosphere. (b) Cyclic volammogram of the PBDTBDD thin film in 0.1 mol/L $Bu_4NPF_6$ acetonitrile solution at a scan rate of 50 mV $s^{-1}$.

**Optical Properties.** Absorption spectra of the polymer are shown in Figure 2a. It is clear that two absorption peaks can be

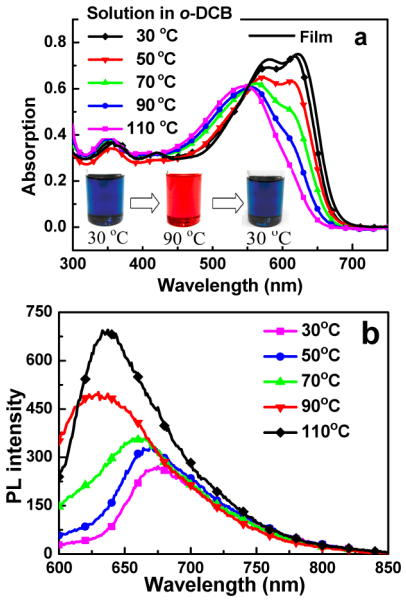


**Figure 2.** (a) UV−vis spectra of PBDTBDD as film and in *o*-DCB solution under different temperature (inset: the color of the solution under different temperature. (b) Temperature-dependent photoluminescence spectra of PBDTBDD in *o*-DCB.

observed in the absorption spectrum of the film. The peak at 581 nm should be attributed to $\pi-\pi^*$ transition along the conjugated backbones of the polymer, while the shoulder peak at 622 nm should be attributed to interchain $\pi-\pi^*$ transition due to the $\pi-\pi$ stacking of the backbones.[21,30] These two absorption peaks can also be observed in *o*-DCB solution at ambient temperature. Considering that PBDTBDD can be readily dissolved into *o*-DCB, it is very interesting to observe such a strong interchain $\pi-\pi^*$ transition shoulder peak in solution state, which means that although the polymer can be dissolved into *o*-DCB, the polymer molecules are strongly aggregated. It was also found that when the *o*-DCB solution was centrifuged under high speed (>$10^4$ rpm/min) for 30 min or/and filtered through a filter ($\phi$ 0.25 $\mu$m), the absorption intensity as well as the peak position of its absorption spectrum has no change, indicating that the size of the aggregations in the solution is very tiny and the solution should be stable enough to perform spin-coating process of device fabrication.

Furthermore, temperature-dependent absorption spectra of the solution were measured to confirm the above finding and


dx.doi.org/10.1021/ma301900h | *Macromolecules* 2012, 45, 9611−9617

presumption. As shown in Figure 2a, it can be seen that when the temperature of the solution was elevated from 30 to 110 °C with an interval of 20 °C, the interchain $\pi-\pi^*$ transition peak at ~618 nm reduced gradually and disappeared finally. Additionally, from 30 to 90 °C, the color of the solution changed from purple to red (see the inset in Figure 2a), and also this thermochromic process is well reversible. Furthermore, temperature-dependent photoluminescence (PL) spectra of the solution were measured (see Figure 2b) to provide more information for the thermochromic phenomenon of the solution. It is clear that when the solution of the polymer was heated up from 30 to 110 °C, the PL emission peak shifted from 670 to 630 nm, while the intensity of the emission increased distinctly. These results from absorption and PL measurements indicate that PBDTBDD has strong aggregation in *o*-DCB solution, and the aggregation can be eliminated at ~110 °C.[31]

**Computational Study.** Quantum chemistry calculation by density functional theory (DFT)[31] at the B3LYP/6-31G level was employed to demonstrate the molecular conformation and the electronic structure of PBDTBDD. As shown in Figure 3,

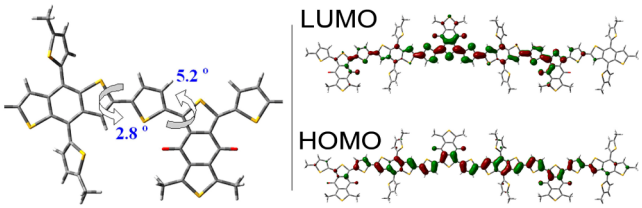


**Figure 3.** Molecular conformation and the frontier molecular orbital surfaces of PBDTBDD.

the conjugated backbone of PBDTBDD has excellent planarity, and the dihedral angels of BDT−thiophene and BDD−thiophene are 2.8° and 5.2°, respectively. The electron density in the HOMO wave function is delocalized over the whole conjugated backbone of the polymer; the electron density associated with the LUMO is mainly localized to the BDD unit with extension onto the whole conjugated backbone units. These two observations from the DFT calculation, i.e., the good planarity and the well delocalized HOMO wave function of the PBDTBDD trimer, give good interpretations for the strong aggregation of PBDTBDD in solution state due to interchain $\pi-\pi$ interaction.[21]

**Photovoltaic Properties.** Polymer solar cells were fabricated using PBDTBDD as electron donor and $PC_{61}BM$ as electron acceptor. The device structure is ITO/PEDOT:PSS/PBDTBDD:$PC_{61}BM$/Ca/Al. Different D/A ratios (PBDTBDD:$PC_{61}BM$, w/w), 1:0.6, 1:1 and 1:2, were scanned. *o*-DCB was used as solvent to make the solutions; ~3% 1,8-diiodooctane (DIO) (DIO/*o*-DCB, v/v) was added to the solutions prior to the spin-coating process to get better photovoltaic performance. The solutions used in D/A ratio scanning were prepared under ambient temperature (ca. 30 °C). The *J*−*V* curves of the devices are shown in Figure 4, and the detailed photovoltaic data are listed in Table 1. It can be seen that the optimum D/A ratio for PBDTBDD/$PC_{61}BM$ blend is 1:1, and a power conversion efficiency (PCE) value of 6.67% was obtained under this condition.

External quantum efficiency (EQE) curves of the devices with different D/A ratios are shown in Figure 5a. The difference between the measured short current density ($J_{sc}$)

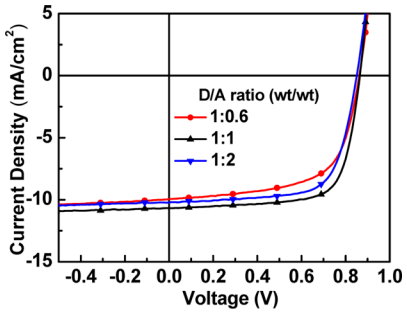


**Figure 4.** *J*−*V* curves of the PSCs based on PBDTBDD/$PC_{61}BM$ with different donor/acceptor ratios (1:0.6, 1:1, 1:2) under the illumination of AM 1.5G, 100 mW/cm².

**Table 1. Photovoltaic Results of the PSCs Based on PBDBDD/$PC_{61}BM$ under the Illumination of AM 1.5G 100 mW/cm²** [a]

| D/A ratio | $V_{oc}$ (V) | $J_{sc}$ (mA/cm²) | FF (%) | PCE (%) | thickness (nm) |
|---|---|---|---|---|---|
| 1:0.6 | 0.86 | 9.95 | 63.50 | 5.44 | 110 |
| 1:1 | 0.86 | 10.68 | 72.27 | 6.67 | 102 |
| 1:2 | 0.85 | 8.95 | 72.29 | 5.50 | 113 |

[a]The solutions of the D/A blends were prepared under 30 °C.

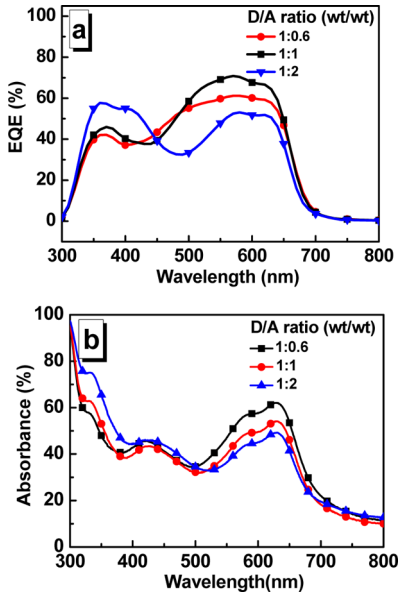


**Figure 5.** (a) EQE curves of the PSCs based on PBDTBDD:$PC_{61}BM$ with different D/A ratios and (b) absorption spectra of their active layers.

values and the current density values calculated by the EQE curves and the standard solar spectrum is within 4%, suggesting the photovoltaic measurements in this work are reliable. Furthermore, the absorption spectra of the blends with different D/A ratios are provided in Figure 5b. Obviously, the blend film with low $PC_{61}BM$ content (D/A = 1:0.6) showed stronger absorbance in the long wavelength direction, while the device with D/A ratio = 1:0.6 only exhibited moderate EQE in this range. On the contrary, the blend with D/A ratio = 1:1 showed moderate absorbance in the range from 500 to 700 nm, but the device based on this blend exhibited higher EQE. The comparison between the EQE curves and the absorption


dx.doi.org/10.1021/ma301900h | *Macromolecules* 2012, 45, 9611−9617

spectra reveals that the device with the optimum D/A ratio can utilize the absorbed sunlight more efficiently.

As mentioned above, PBDTBDD shows strong aggregation in *o*-DCB solution under ambient temperature, and the aggregation can be eliminated by heating up. Although the thermochromic process of PBDTBDD solution is reversible, the aggregation size in the solution might be changed after the heating and cooling cycle. Consequently, D/A blend films with different morphology might be obtained by using the D/A solutions treated by different heating up temperature. In order to investigate the influence of the heating up process during the solution preparation on device performance as well as on morphology of the blend, two kinds of devices (devices A and B as demonstrated in Chart 1) were prepared in parallel. It should be emphasized that the D/A blend films for both of the two devices are spin-coated under ambient temperature (ca. 30 °C) in the glovebox. The *J*−*V* curves of these two devices are shown in Figure 6, and the detailed parameters are collected in Table

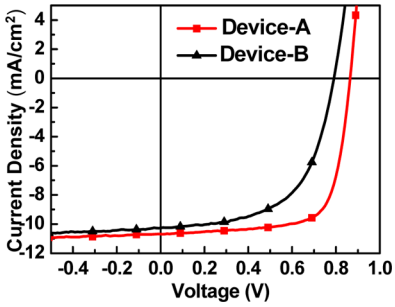


**Figure 6.** *J*−*V* curves of devices A and B. Device A: the solution of active layer materials was prepared under 30 °C. Device B: the solution of active layer materials was prepared under 90 °C.

**Table 2. Photovoltaic Results of the PSCs Based on PBDBDD/$PC_{61}BM$ under the Illumination of AM 1.5G 100 mW/cm²**

| | temp[a] (°C) | $V_{oc}$ (V) | $J_{sc}$ (mA/cm²) | FF (%) | PCE (%) |
|---|---|---|---|---|---|
| device A | 30 | 0.86 | 10.68 | 72.27 | 6.67 |
| device B | 90 | 0.79 | 10.27 | 58.18 | 4.72 |

[a]The temperature used for making the solutions of the D/A blends.

2. It is clear that these two devices show very similar $J_{sc}$ values. However, open circuit voltage ($V_{oc}$) and fill factor (FF) of the devices reduced obviously when higher temperature was employed in the D/A solution preparation process. As a result, device B shows a PCE of 4.72%, which is 30% lower than that of device A.

**Morphology Study.** GIXD has been widely used to characterize the formation of ordered structures within thin films. In this study, this technique is used to examine the crystalline structure of the D/A blends in devices A and B. Figure 7a shows the out-of-plane and in-plane profiles of the blends in these two kinds of devices. Interestingly, although these two kinds of devices exhibit much different photovoltaic performance, the GIXD profiles of the two blend films are almost the same. In both two blend films, a clear peak at 0.29 $Å^{-1}$ can be observed (corresponding to a *d*-spacing of 18.4 Å), indicating that the crystallinity of this polymer is good. In order to analyze the crystalline structure of the two blends, the curves

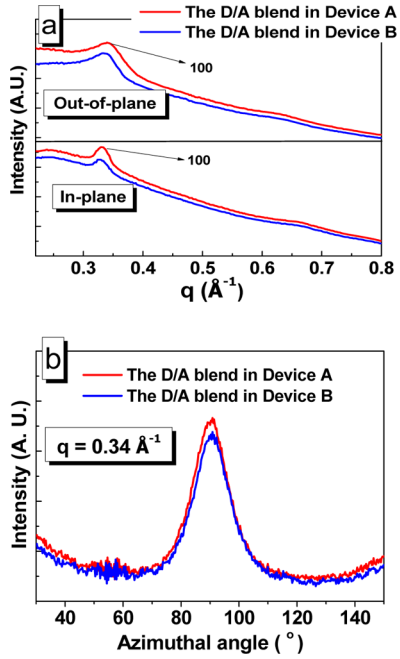


**Figure 7.** (a) GIXD curves (out-of-plane and in-plane) and (b) azimuthal angle of the blend films of devices A and B.

of the azimuthal angle of the two blend films are also provided in Figure 7b, and it is quite clear that the two curves are almost identical (with a peak at 90.7°). On the basis of the information obtained from GIXD analysis, it can be concluded that the temperature used in D/A blend solution preparation of has little influence on molecular orientation as well as crystallinity of the blend film.

Atomic force microscopy (AFM) measurements were carried out to study the surface morphology of the thin film blends. As shown in Figures 8a and 8d, the active layer of devices A and B

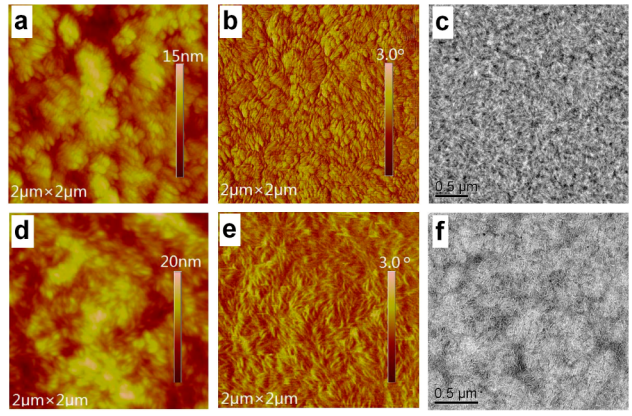


**Figure 8.** AFM phase images (a, d), topographies (b, e), and TEM images (c, f) of devices A and B, respectively.

shows similar properties in topography, i.e., the mean-square surface roughness ($R_q$) of the blend films of devices A and B are 3.57 and 3.89 nm, respectively. However, the shapes of the domains in devices A and B are very different. In the blend film of device A, small domains with irregular shapes can be seen in the whole phase image (Figure 8b), while in the blend film of device B, fibril-like domains permeate in the whole image (see Figure 8e). Furthermore, transmission electron microscopy


dx.doi.org/10.1021/ma301900h | *Macromolecules* 2012, 45, 9611−9617

(TEM) was used to give a real space image of the phase-separated morphology of the blends, and the TEM images of the D/A blends of these two devices are provided in Figures 8c and 8f. In Figure 8c, short fibril domains can be observed in the D/A blend of device A, and the fibrils permeate evenly in the whole region of the image. However, as we can see, bigger size fibrils (over 100−200 nm in length) as well as bigger polymer domains can be clearly observed in the blend film of device B (see Figure 8f) and also the fibrils in device B are aggregated together, and thus larger polymer and PCBM domains are formed. On the basis of the observation from AFM and TEM measurements, it can be concluded that since the polymer shows strong aggregation in *o*-DCB under ambient temperature and the aggregation can be eliminated by heating up, the polymer can be molecular-level dispersed in the solvent under high temperature, and the heating and cooling process can be seen as an annealing process in solution and hence the size of the aggregations in solution might be increased. When the solution with bigger aggregations was spin-casted, larger polymer and $PC_{61}BM$ domains were formed[23−26] which limit exciton diffusion as well as charge separation. As a result, the current density of device B is lower than that of device A. Additionally, the phenomenon of reducing $V_{oc}$ by increasing domain sizes in this work is quite similar as the reported results.[25,26] Although the blends with different morphological properties show almost identical absorption bands, Fermi levels of the polymer and $PC_{61}BM$ aggregations can be affected by changing their sizes; i.e., the larger polymer and PCBM domains in device B may cause lowing of effective LUMO level of PCBM cluster and elevating of HOMO level of the polymer aggregation,[32,33] and thus device B shows lower $V_{oc}$ than device A.

## ■ CONCLUSIONS

A new conjugated polymer named as PBDTBDD was designed, synthesized, and applied in PSCs, and this new polymer exhibits promising photovoltaic properties. A PCE of 6.67% was recorded in the PSC device based on PBDRBDD/$PC_{61}BM$, and this is a remarkable result for the PSCs using $PC_{61}BM$ as electron acceptor. PBDTBDD shows a strong aggregation effect in solution state, and the study indicates that photovoltaic properties of the D/A blend films can be affected by the processing temperature used in solution preparation. By using GIXD, AFM, and TEM, we found that although the temperature used in making the solution has little influence on molecular orientation as well as crystallinity of the D/A blend, it plays an important role in forming appropriate domain size in the blend. Since the solution preparation of active layer materials is one of the indispensable processes for device fabrication and less attention has been paid for the temperature used in this process, this work provides a good example to reveal the correlation between the morphology of the blend films and the processing temperature of the solution. Furthermore, the study in this work suggests an interesting and feasible approach to modulate domain size in blend films of polymer solar cells.

## ■ EXPERIMENTAL SECTION

**Materials.** (4,8-Bis(5-(2-ethylhexyl)thiophen-2-yl)benzo[1,2-*b*:4,5-*b*′]dithiophene-2,6-diyl) bis(trimethylstannane) (BDT) and 2,5-bis(2-ethylhexyl)thiophene were purchased from Solarmer Materials Inc.; $Pd(PPh_3)_4$ was purchased from Frontiers Scientific Inc. All of these chemicals were used as received. The other materials were common commercial level and used as received.

**Instruments.** $^1H$ and $^{13}C$ NMR spectra were measured on a Bruker arx-400 spectrometer in $CDCl_3$ at 293 K. UV−vis absorption spectra were taken on a Hitachi U-3100 UV−vis spectrophotometer. PL spectra were taken on a Cary Eclipse fluorescence spectrophotometer. The molecular weight of polymer was measured by the GPC method, and polystyrene was used as a standard by using chloroform as eluent. TGA measurement was performed on a TA Instruments, Inc., TGA-2050. The electrochemical cyclic voltammetry was conducted on a CHI650D electrochemical workstation with Pt disk, Pt plate, and $Ag/Ag^+$ electrode as working electrode, counter electrode, and reference electrode, respectively, in a 0.1 M tetrabutylammonium hexafluorophosphate ($Bu_4NPF_6$)−acetonitrile solution. GIXD measurements were performed at 1W1A diffuse scattering experimental station of Beijing Synchrotron Radiation Facility (BSRF), Institute of High Energy Physics, Chinese Academy of Sciences. AFM measurement of the surface morphology of samples was conducted on a Nanoscope III (Vecco) in tapping mode with a 2 $\mu$m scanner. TEM was performed using a JEOL 2200FS instrument at 160 kV accelerating voltage. EQE was measured by the Solar Cell Spectral Response Measurement System QE-R3011 (Enli Technology Ltd., Taiwan). The light intensity at each wavelength was calibrated with a standard single-crystal Si photovoltaic cell.

**Fabrication of Polymer Solar Cells.** Polymer solar cell devices were fabricated under conditions as follows: After spin-coating a ∼30 nm layer of poly(3,4-ethylenedioxythiophene):poly(styrenesulfonate) (PEDOT:PSS) onto a precleaned indium−tin oxide (ITO)-coated glass substrates, the polymer/PCBM blend solution which stirred for 5 h under the two different temperature (30 and 90 °C) was spin-coated. The concentration of the polymer:PCBM blend solution used in this study for spin-coating was 12.5 mg/mL (polymer/*o*-dichlorobenzene), and *o*-dichlorobenezene was used as the solvent. The additive, 1,8-diiodooctane (DIO) with 3% volume ratio, was added prior to spin-coating process. The devices were completed by evaporating Ca/Al metal electrodes with an area of 4 $mm^2$ as defined by masks. The current−voltage curves are measured under 100 mW $cm^{-2}$ standard AM 1.5G spectrum using a XES-70S1 (SAN-EI Electric Co., Ltd.) solar simulator (AAA grade, 70 mm × 70 mm photobeam size). The 2 cm × 2 cm monocrystalline silicon reference cell (SRC-1000-TC-QZ) was purchased from VLSI Standards Inc.

**Synthesis.** *2,5-Dibromothiophene-3,4-dicarboxylic Acid, Compound 1.* This compound was synthesized by the reported method.[34] MS: $m/z$ = 330. $^{13}C$ NMR ($d_6$-DMSO, 400 MHz), $\delta$ (ppm): 162.5, 135.2, 114.3.

*1,3-Dibromo-5,7-bis(2-ethylhexyl)benzo[1,2-c:4,5-c′]-dithiophene-4,8-dione, Compound 2.* Oxalyl chloride (10 mL) was slowly added to compound **1** (4.95 g, 15 mmol) and DMF (1 drop) in dry dichloromethane (20 mL). The mixture was stirred for 12 h at room temperature. The solvent was removed under vacuum to obtain crude 2,5-dibromothiophene-3,4-dicarbonyl dichloride, which was used for next step without further purification. To a stirred solution of the dicarbonyl dichloride (5.5 g, 15 mmol) and 2,5-bis(2-ethylhexyl)thiophene (4.62 g, 15 mmol) in dry 1,2-dichloroethane, $AlCl_3$ (8 g, 60 mmol) was added in small portions at 0 °C. The mixture was allowed to stir at 0 °C for 30 min and then at room temperature for 3 h. The mixture was poured into ice with 1 mol/L hydrochloric acid and then extracted with $CHCl_3$. The organic layer was collected and the volatile solvent was removed under vacuum. The crude product was purified through a silica gel column with petroleum ether/dichloromethane (5:1 by volume) to give a pale yellow solid (6.3 g, 70%). $^1H$ NMR ($CDCl_3$, 400 MHz), $\delta$ (ppm): 3.31 (m, 4 H), 1.77 (m, 2 H), 1.43−1.26 (m,16 H), 1.40−1.29 (m, 6 H), 0.92−0.86 (m,12 H). $^{13}C$ NMR ($CDCl_3$, 400 MHz), $\delta$ (ppm): 175.5, 155.3, 134.9, 132.8, 119.5, 41.2, 34.0, 32.7, 28.8, 26.0, 23.1, 14.2, 10.9. Elemental analysis calculatd for [$C_{26}H_{34}Br_2O_2S_2$ ]: C, 51.83; H, 5.69. Found: C, 51.67; H, 5.59.

*1,3-Bis(2-ethylhexyl)-5,7-di(thiophen-2-yl)benzo[1,2-c:4,5-c′]-dithiophene-4,8-dione, Compound 3.* $Pd(PPh_3)_4$ (40 mg) was added to a solution of compound **2** (3 mmol,1.8 g) and thimethyl(thiophen-


dx.doi.org/10.1021/ma301900h | *Macromolecules* 2012, 45, 9611−9617

2-yl)stannane (9 mmol, 3.4 g) in 20 mL of toluene. The mixture was refluxed in a nitrogen atmosphere for 12 h. After the removal of the solvent at a reduced pressure, the residue was purified by column chromatography on a silica gel column with petroleum ether/dichloromethane (5:1 by volume) to give an orange/yellow solid (1.73 g, 95%). $^1$H NMR (400 MHz,$CDCl_3$) (ppm): 7.72 (d, 2H), 7.50 (d, 2H), 7.13 (t, 2H), 3.36(m, 4H), 1.77 (m, 2H), 1.43−1.28 (m, 16H), 0.93−0.86 (m, 12H). $^{13}$C NMR (400 MHz, $CDCl_3$) (ppm): 177.7, 153.6, 142.4, 133.4, 133.1, 132.7, 130.5, 129.3, 127.2, 41.3, 33.7, 32.8, 28.8, 26.0, 23.0, 14.2, 10.9. Elemental analysis calculatd for [$C_{34}H_{40}O_2S_4$]: C, 67.06; H, 6.62. Found: C, 67.71; H, 6.76.

*1,3-Bis(5-bromothiophen-2-yl)-5,7-bis(2-ethylhexyl)benzo[1,2-c:4,5-c′]dithiophene-4,8-dione (BDD).* Compound **3** (2.6 mmol, 1.6 g) was added into DMF (20 mL). After the solid dissolved completely, *N*-bromosuccinimide (NBS) (5.3 mmol, 0.95 g) was added in one portion. The reaction mixture was stirred at room temperature for 3 h, water was added into the mixture, the mixture was extracted with $CHCl_3$, and the organic layer was washed with brine and dried over anhydrous sodium sulfate. The solvent was removed at a reduced pressure; the residue was purified by column chromatography on silica gel with petroleum ether/acetic ether (30:1 by volume) to give a red solid (1.17 g, 60%). $^1$H NMR (400 MHz, $CDCl_3$) (ppm): 7.39 (d, 2H), 7.03 (d, 2H), 3.27 (m, 4H), 1.74(m, 2H), 1.41−1.32 (m, 16H), 0.94−0.90 (m, 12H). $^{13}$C NMR (400 MHz, $CDCl_3$) (ppm): 177.1, 153.8, 141.2, 134.6, 132.5, 131.5, 130.1, 129.5, 118.4, 41.1, 33.7, 32.9, 29.0, 26.1, 23.1, 14.3, 10.9. Elemental analysis calculatd for [$C_{34}H_{38}Br_2O_2S_4$ ]: C, 53.26; H, 5.00. Found: C, 53.28; H, 5.02.

*Polymerization of PBDTBDD.* BDD (271 mg, 0.3 mmol) and BDT (230 mg, 0.3 mmol) were dissolved in 10 mL of toluene; the solution was flushed with argon for 5 min, and then 25 mg of $Pd(PPh_3)_4$ was added into the solution. The mixture was again flushed with argon for 20 min. The reaction solution was heated to reflux for 11.5 h. The reaction mixture was cooled to room temperature and added dropwise to 100 mL of methanol. The precipitate was collected and further purified by Soxhlet extraction with methanol, hexane, and chloroform in sequence. The chloroform fraction was concentrated and added dropwise into methanol. Subsequently, the precipitates were collected and dried under vacuum overnight to get polymer as solid (270 mg, 75% yield). $^1$H NMR ($CDCl_3$, 400 MHz), $\delta$ (ppm): 8.20−7.50 (br, 2 H), 7.10−6.10 (br, 8 H), 4.12−2.50 (br, 8 H), 2.50−0.20 (br, 60 H). Elemental analysis calculatd for [$C_{68}H_{78}O_2S_8$ ]: C, 68.99; H, 6.64; S, 21.67. Found: C, 68.43; H, 6.45; S, 21.15. The weight-average molecular weight ($M_w$) and the polydispersity index (PDI) estimated by GPC are 13.5K and 1.18, respectively.

## AUTHOR INFORMATION


### Corresponding Author

*E-mail: hjhzlz@iccas.ac.cn (J.H.); tanzhanao@ncepu.edu.cn (Z.T.).

### Author Contributions

§D. Qian and L. Ye contributed equally to this work.


### Notes

The authors declare no competing financial interest.

## ACKNOWLEDGMENTS

This work was supported by the National Natural Science Foundation of China (No. 51173040), Project 863 (2011AA050523), and Chinese Academy of Sciences. Beijing Synchrotron Radiation Facility (BSRF) is acknowledged for the grazing incidence X-ray diffraction measurements.

## REFERENCES


(1) Chen, H. Y.; Hou, J. H.; Zhang, S. Q.; Liang, Y. Y.; Yang, G. W.; Yang, Y.; Yu, L. P.; Wu, Y.; Li, G. *Nat. Photonics* **2009**, *3*, 649−653.

(2) Park, S. H.; Roy, A.; Beaupré, S.; Cho, S.; Coates, N.; Moon, J. S.; Moses, D.; Leclerc, M.; Lee, K.; Heeger, A. J. *Nat. Photonics* **2009**, *3*, 297−302.

(3) (a) Zhao, G. J.; He, Y. J.; Li, Y. F. *Adv. Mater.* **2010**, *22*, 4355−4358. (b) Tan, Z. A.; Zhang, W. Q.; Zhang, Z. G.; Qian, D. P.; Huang, Y.; Hou, J. H.; Li, Y. F. *Adv. Mater.* **2012**, *24*, 1476−1481.

(4) Holcombe, T. W.; Douglas, J. D.; Woo, C. H.; Beaujuge, P. M.; Fréchet, J. M. J. *J. Am. Chem. Soc.* **2010**, *132*, 7595−7597.

(5) Li, X. H.; Choy, W. C. H.; Huo, L. J.; Xie, F. X.; Sha, W. E. I.; Ding, B. F.; Guo, X.; Li, Y. F.; Hou, J. H.; You, J. B.; Yang, Y. *Adv. Mater.* **2012**, *24*, 3046−3052.

(6) Hou, J. H.; Chen, H. Y.; Zhang, S. Q.; Li, G.; Yang, Y. *J. Am. Chem. Soc.* **2008**, *130*, 16144−16145.

(7) Hou, J. H.; Chen, H. Y.; Zhang, S. Q.; Chen, R. I.; Yang, Y.; Wu, Y.; Li, G. *J. Am. Chem. Soc.* **2009**, *131*, 15586−15587.

(8) Huo, L. J.; Hou, J. H.; Zhang, S. Q.; Chen, H. Y.; Yang, Y. *Angew. Chem., Int. Ed.* **2010**, *49*, 1500−1503.

(9) Zou, Y. P.; Najari, A.; Berrouard, P.; Beaupré, S.; Réda Aïch, B.; Tao, Y.; Leclerc, M. *J. Am. Chem. Soc.* **2010**, *132*, 5330−5331.

(10) Huo, L. J.; Zhang, S. Q.; Guo, X.; Xu, F.; Li, Y. F.; Hou, J. H. *Angew. Chem., Int. Ed.* **2011**, *50*, 9697−9702.

(11) Huang, Y.; Guo, X.; Liu, F.; Huo, L. J.; Chen, Y. N.; Russell, T. P.; Han, C. C.; Li, Y. F.; Hou, J. H. *Adv. Mater.* **2012**, *24*, 3383−3389.

(12) Amb, C. M.; Chen, S.; Graham, K. R.; Subbiah, J.; Small, C. E.; So, F.; Reynolds, J. R. *J. Am. Chem. Soc.* **2011**, *133*, 10062−10065.

(13) Chu, T. Y.; Lu, J. P.; Beaupré, S.; Zhang, Y. G.; Pouliot, J. R.; Wakim, S.; Zhou, J. Y.; Leclerc, M.; Li, Z.; Ding, J. F.; Tao, Y. *J. Am. Chem. Soc.* **2011**, *133*, 4250−4253.

(14) Price, S. C.; Stuart, A. C.; Yang, L. Q.; Zhou, H. X.; You, W. *J. Am. Chem. Soc.* **2011**, *133*, 4625−4631.

(15) Lee, J.; Ma, W.; Brabec, C.; Yuen, J.; Moon, J.; Kim, J.; Lee, K.; Bazan, G.; Heeger, A.; Kwan Lee, Jae; Ma, W. L.; Brabec, C. J.; Yuen, J.; Moon, J. S.; Kim, J. Y.; Lee, K.; Bazan, G. C.; Heeger, A. J. *J. Am. Chem. Soc.* **2008**, *130*, 3619−3623.

(16) Li, G.; Shrotriya, V.; Huang, J.; Yao, Y.; Moriarty, T.; Emery, K.; Yang, Y. *Nat. Mater.* **2005**, *4*, 864−868.

(17) Yang, X. N.; Loos, J. *Macromolecules* **2007**, *40*, 1353−1362.

(18) Ye, L.; Zhang, S. Q.; Ma, W.; Fan, B. H.; Guo, X.; Huang, Y.; Ade, H.; Hou, J. H. *Adv. Mater.* **2012**, DOI: 10.1002/adma.201202855.

(19) (a) Yao, Y.; Hou, J. H.; Xu, Z.; Li, G.; Yang, Y. *Adv. Funct. Mater.* **2008**, *18*, 1783−1789. (b) Guo, X.; Cui, C. H.; Zhang, M. J.; Huo, L. J.; Huang, Y.; Hou, J. H.; Li, Y. F. *Energy Environ. Sci.* **2012**, 2012, *5*, 7943-7949.

(20) Ma, W. L.; Yang, C. Y.; Gong, X.; Lee, K.; Heeger, A. J. *Adv. Funct. Mater.* **2005**, *16*, 1617−1622.

(21) Chen, H. Y.; Hou, J. H.; Hayden, A. E.; Yang, H.; Houk, K. N.; Yang, Y. *Adv. Mater.* **2010**, *22*, 371−375.

(22) Rughooputh, S. D. D. V.; Hoytta, S.; Heeger, A. J.; Wudl, F. *J. Polym. Sci., Polym. Phys.* **1987**, *25*, 1071−1078.

(23) Nguyen, T. Q.; Doan, V.; Schwartz, B. J. *J. Chem. Phys.* **1999**, *110*, 4068−4078.

(24) Nguyen, T. Q.; Martini, I. B.; Liu, J.; Schwartz, B. J. *J. Phys. Chem. B* **2000**, *104*, 237−255.

(25) Nguyen, T. Q.; Kwong, R. C.; Thompson, M. E. *Appl. Phys. Lett.* **2000**, *76*, 2454−2456.

(26) Huang, Y.; Cheng, H.; Han, C. C. *Macromolecules* **2010**, *43*, 10031−10037.

(27) Ie, Y.; Huang, J.; Uetani, Y.; Karakawa, M.; Aso, Y. *Macromolecules* **2012**, *45*, 4564−4571.

(28) Li, Y. F.; Cao, Y.; Gao, J.; Wang, D. L.; Yu, G.; Heeger, A. J. *Synth. Met.* **1999**, *99*, 243−248.

(29) (a) Sun, Q. J.; Wang, H. Q.; Yang, C. H.; Li, Y. F. *J. Mater. Chem.* **2003**, *13*, 800−806. (b) Hou, J. H.; Tan, Z. A.; Yan, Y.; He, Y. J.; Yang, C. H.; Li, Y. F. *J. Am. Chem. Soc.* **2006**, *128*, 4911−4916.

(30) (a) Clark, J.; Chang, J. F.; Spano, F. C.; Friend, R. H.; Silva, C. *Appl. Phys. Lett.* **2009**, *94*, 163306. (b) Spano, F. C. *J. Chem. Phys.* **2005**, *122*, 234701. (c) Clark, J.; Silva, C.; Friend, R.; Spano, F. *Phys. Rev. Lett.* **2007**, *98*, 206406. (d) Clark, J.; Silva, C.; Friend, R. H.; Spano, F. C. *J. Chem. Phys.* **2012**, *136*, 184901.

(31) Parr, R. G.; Weitao, Y. *Density Functional Theory of Atoms and Molecules*; Oxford University Press: New York, 1989.

(32) Vandewal, K.; Gadisa, A.; Oosterbaan, W. D.; Bertho, S.; Banishoeib, F.; Severen, I. V.; Lutsen, L.; Cleij, T. J.; Vanderzande, D.; Manca, J. V. *Adv. Funct. Mater.* **2008**, *18*, 2064−2070.
(33) Veldman, D.; Ipek, O.; Meskers, S. C. J.; Sweelssen, J.; Koetse, M. M.; Veenstra, S. C.; Kroon, J. M.; Bavel, S. S.; Loos, J.; Janssen, R. A. J. *J. Am. Chem. Soc.* **2008**, *130*, 7721−7735.
(34) Cui, C. H.; Fan, X.; Guo, X.; Zhang, M. J.; He, Y. J.; Zhan, X. W.; Li, Y. F. *Polym. Chem.* **2012**, *3*, 99−104.